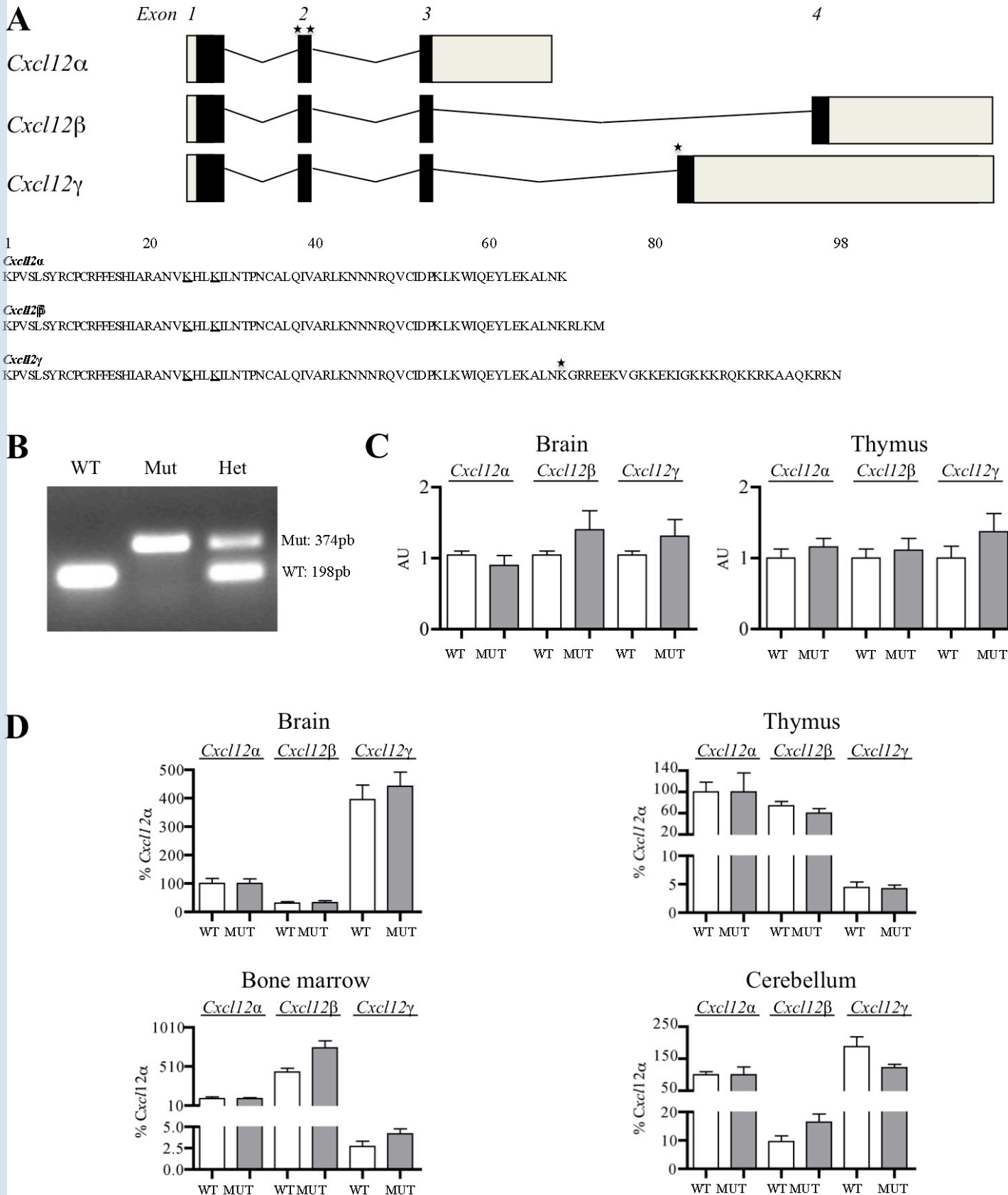
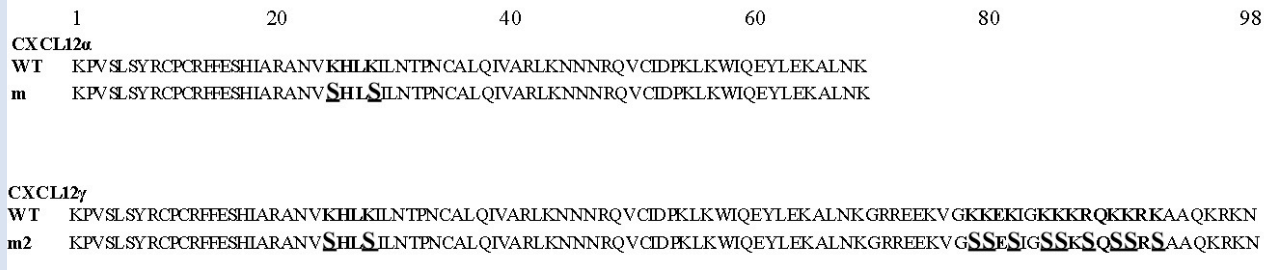
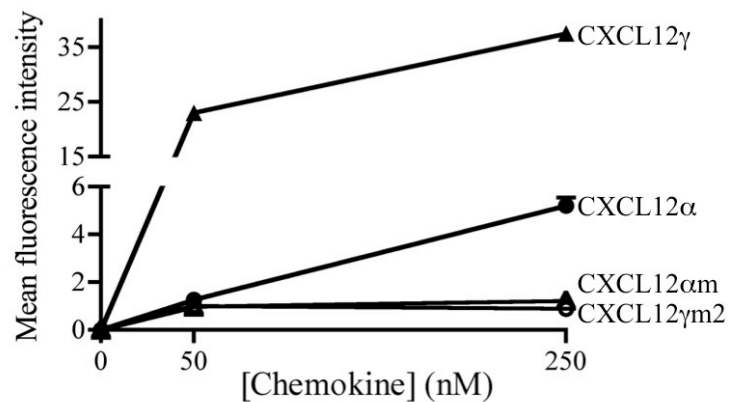
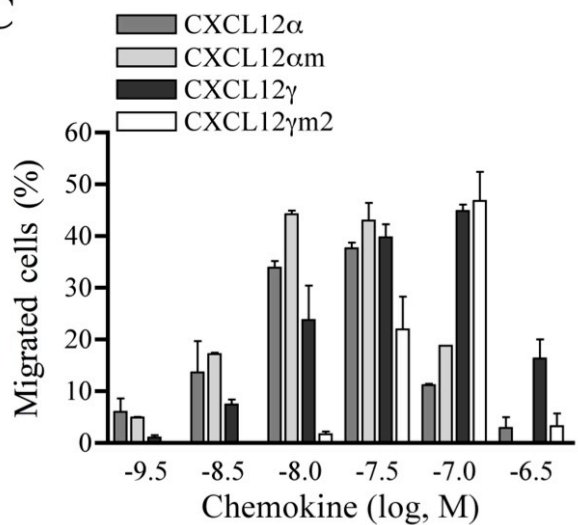
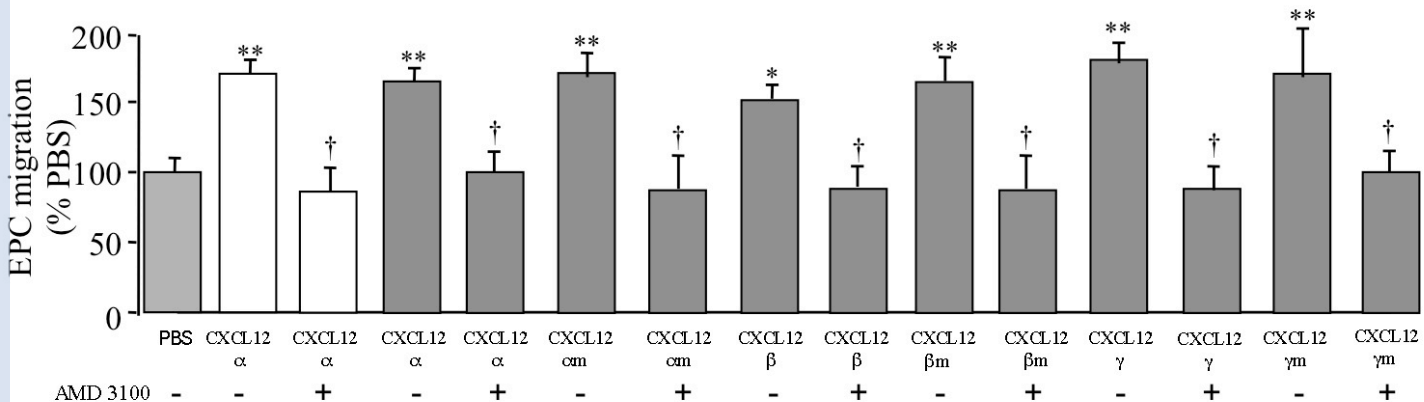


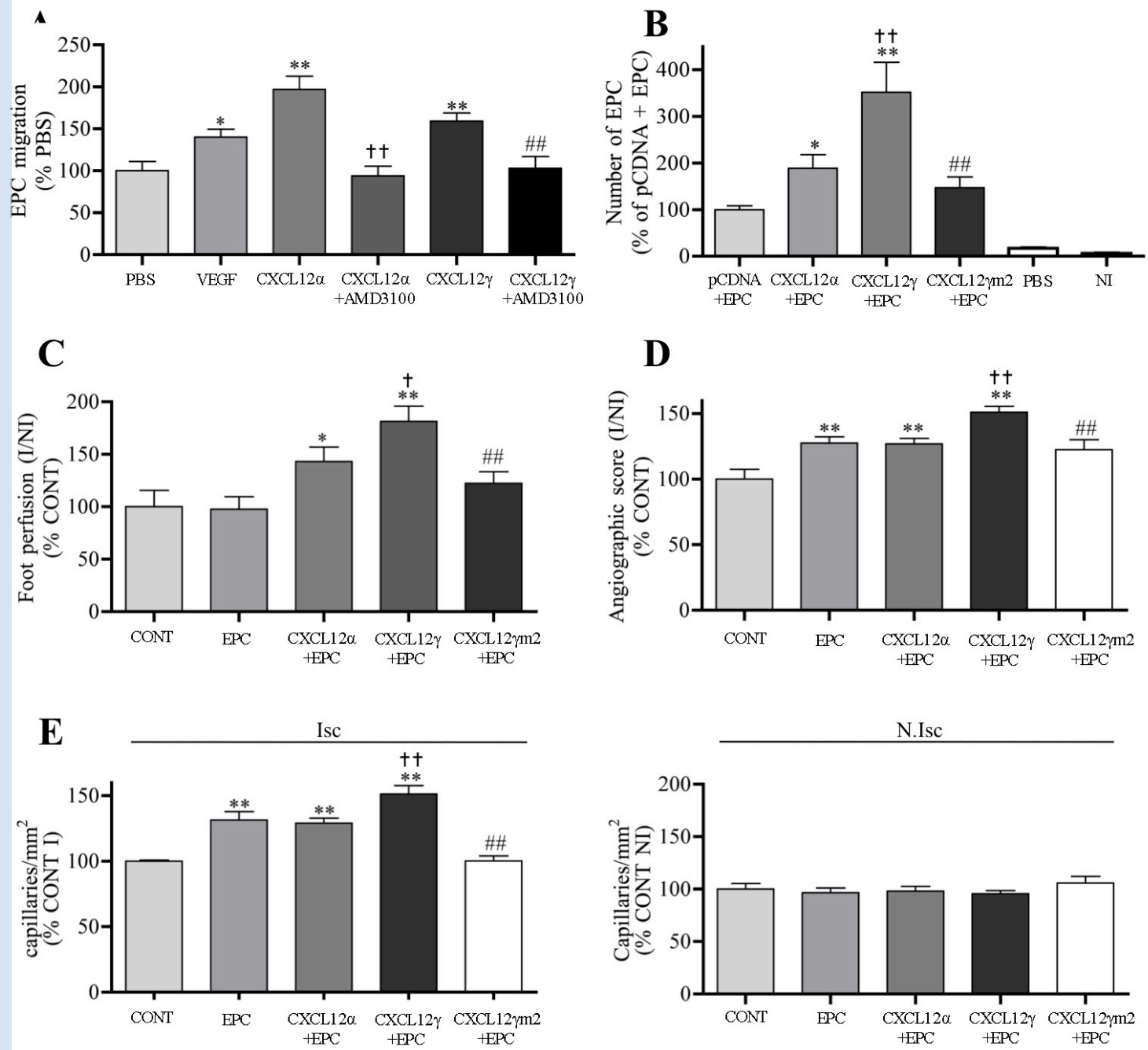
# Supplemental Material



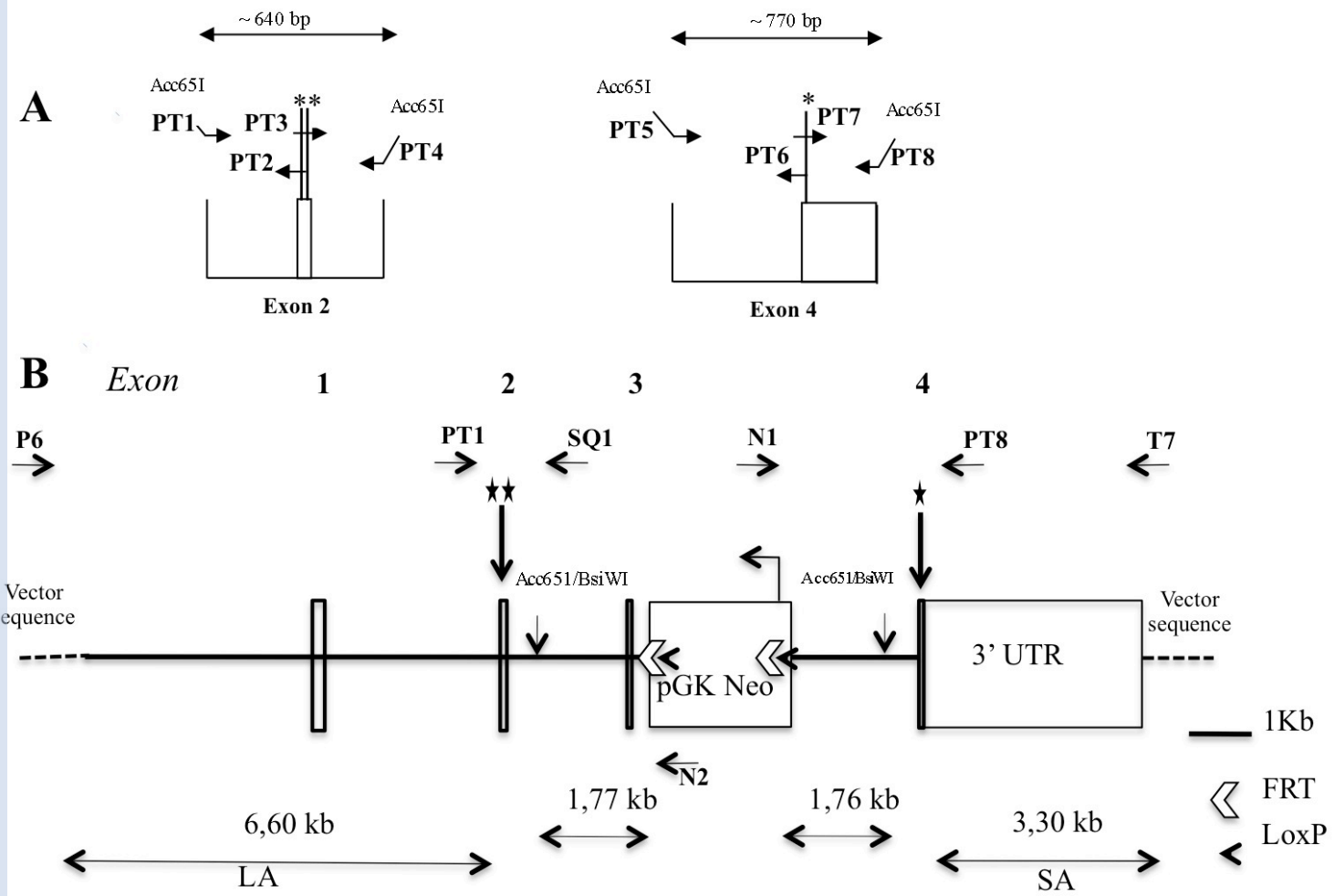
**Supplementary Figure 1. Characterization of *Cxcl12*<sup>Gagtm/Gagtm</sup> animals.** (A) Schematic diagram of *Cxcl12* isoforms structures and sequence alignment of the corresponding mature proteins. Mutations introduced in *Cxcl12*<sup>Gagtm</sup> are indicated (stars). In the amino-acid sequence the substituted residues corresponding to mutations are underlined. The incorporation of the non-sense mutation in the open reading frame of *Cxcl12γ* generates a truncated protein of 68Aa-length identical to *Cxcl12α*, which last aminoacid (K68) is marked by a star. (B) PCR amplification on genomic DNA from wild type (WT), *Cxcl12*<sup>Gagtm/wt</sup> (Het) and *Cxcl12*<sup>Gagtm/Gagtm</sup> (Mut) animals. (C-D) Real-time PCR analysis of *Cxcl12* products. (C) RNA expression levels of each isoform normalized to HPRT in brain and thymus tissues from WT and *Cxcl12*<sup>Gagtm/Gagtm</sup> animals. (D) mRNA levels of each *Cxcl12* isoform were normalized to that of *Cxcl12α*.

**A****B****C****D**

**Supplementary Figure 2. Functional properties of WT and HS-binding mutant CXCL12 used for post-ischemic revascularization treatment or expressed from *Cxcl12<sup>Gagtm</sup>* animals.** (a) Sequence alignment of CXCL12 WT and mutant chemokines used in experiments described in b and c. In bold, HS-binding motifs; underlined, substituted amino acids. (b) Cell surface (CHO cells) binding activity and (c) chemotactic properties of synthetic WT and HS-binding mutants CXCL12 $\alpha$ m and CXCL12 $\gamma$ m2 assessed in CD4+ T lymphocytes. (d) Quantitative evaluation of EPC migration through transwell membrane in response to treatment with supernatant of HEK293 T transfected cells with cDNA coding either for WT or mutant isoforms isolated from *Cxcl12<sup>Gagtm</sup>* animals. CXCL12 content in supernatants was measured by ELISA and for each WT/mutant couple equal amounts (ranging from 0,5 to 1nM) were used. Open bars: synthetic CXCL12 $\alpha$ , 1nM. AMD3100 (5 $\mu$ M) is a low molecular, synthetic CXCR4 antagonist. PBS, Phosphate buffered saline. \*\*p<0.01 versus PBS, † p<0.05 versus conditions without AMD3100. n = 10 per group, representative of 2 independent experiments.



**Supplementary Figure 3. CXCL12 $\gamma$  controls EPC infiltration in ischemic tissues.** (a) Quantitative evaluation of EPC migration through transwell membrane in response to VEGF, CXCL12 $\alpha$  or CXCL12 $\gamma$ , in presence or absence of the synthetic CXCR4 antagonist, AMD3100 (5 $\mu$ M). n = 6 to 8 per group, representative of 2 independent experiments. \*p<0.05, \*\*p<0.01, \*\*\*p<0.001 versus PBS, ††† p<0.001 versus CXCL12 $\alpha$ , ## p<0.01 versus CXCL12 $\gamma$ . (b) Number of CFSE-stained human EPC (EPC) in the ischemic leg of C57BL/6 mice treated with intramuscular administration of cDNA expression vector encoding CXCL12 $\alpha$ , CXCL12 $\gamma$  or CXCL12 $\gamma$ m2, 4 days after the onset of ischemia. Quantitative evaluation of foot perfusion (c), microangiography (d) and capillary density (e), 14 days after ischemia in C57BL/6 mice treated with intravenous administration of EPC only or along with intramuscular cDNA expression vector encoding CXCL12 $\alpha$ , CXCL12 $\gamma$  or CXCL12 $\gamma$ m2. Empty DNA plasmid (CONT). Values are mean  $\pm$  SEM. n = 10 per group, representative of 2 independent experiments. 10 possible comparisons for Bonferroni correction, a value of p<0.005 was considered significant. \*p<0.005, \*\*p<0.001, versus CONT, † p<0.005, †† p<0.001 versus CXCL12 $\alpha$ +EPC, ##p<0.001 versus CXCL12 $\gamma$  + EPC.



**Supplementary Figure 4. Construction and sequencing validation of point mutation targeting vector of *Cxcl12*.** (a) Point mutations in 2<sup>nd</sup> and 4<sup>th</sup> exons were generated by 3-step PCR mutagenesis using PT1-PT4 and PT5-PT8 primers. The PCR fragments carrying mutations were then used to replace the correspondent wild type sequence using conventional sub cloning methods. (b) The boundaries of the two homology arms (LA , SA) were confirmed by sequencing with P6 and T7 primers that read through both sides of the backbone vector. The floxed Neo cassette was confirmed by sequencing with N1 and N2 primers that read from the 5'- and 3'- ends of the Neo cassette, respectively, into the genomic sequences. The mutations were confirmed by sequencing with PT1, SQ1 and PT8 primers. The sequencing results also proved that no other mutations were introduced into exon 2 and exon 4 before the natural stop codon.

#### Primers used to generate the point mutations (mutations are in bold and underlined)

PT1 (**Acc65I**): 5'- ACTTGGTACCAACTTCTGTAACCATTCTGC -3'

PT2: 5'- AGACAGATGCGAGACGTTGGCTCTGGCGATGTGGCTC -3'

PT3: 5'- ACATGCCAGAGCCAACGTTCGCATCTGTTCTATCCTAACACTCCAAACTGTG -3'

PT4 (**Acc65I**): 5'- ACTTGGTACCCTCTGAGCAAGTGAGTGCAAGTG -3'

PT5 (**Acc65I**): 5'- ACTTGGTACCCTCTAGAACAATTCAGTTATCC -3'

PT6: 5'- CTACCCTAGATAAAATTAGTAGAACCC -3'

PT7: 5'- GTTCTACTAATTTCTAAGGTAGGGCGCAGAGAAGAAAAAGTGG -3'

PT8 (**Acc65I**): 5'- ACTTGGTACCAAGAGTTACCGTCAGGTTGAGC -3

#### Sequencing Primer Sequences

Primer N1 5' -TGCAGGGCCAGAGGCCACTTGTGTAGC- 3'

Primer N2 5' -TCCCTCGTGTCTTACGGTATCG- 3'

Primer P6 5' -GAGTGCACCATATGGACATATTGTC- 3'

Primer T7 5' -TAATGCAGGTTAACCTGGCTTATCG- 3'

Primer PT1 5' -ACTTGGTACCAACTTCTGTAACCATTCTGC- 3'

Primer SQ1 5' -ACAGGACACATCTGCCAAGTC- 3'

Primer PT8 5' -ACTTGGTACCAAGAGTTACCGTCAGGTTGAGC- 3'